VIP Proton Mobility

DOI: 10.1002/anie.201104883

Enhancement of Proton Mobility in Extended-Nanospace Channels**

*Hiroyuki Chinen, Kazuma Mawatari, Yuriy Pihosh, Kyojiro Morikawa, Yutaka Kazoe, Takehiko Tsukahara, and Takehiko Kitamori**

Currently, the microfluidics research field is rapidly moving its focus to the "extended nanospace", in the 10^1–10^3 nm scale. In the range of 10^{-1}–10^1 nm, many unique properties of liquids have already been reported. These properties include molecular motions,[1] phase transition,[2] and also ion transport in the extended nanospace.[3] In particular, proton transport in the extended nanospace has attracted general interest for the purpose of understanding water properties. Recently developed fundamental technologies have enabled the discovery of many unique liquid properties,[4,5] including ion enrichment[6] and viscosity increase.[7,8]

Recently, our group reported on the enhancement of the proton-transfer rate. The work was based on measurements of the relaxation rate of water molecules confined in two-dimensional extended-nanospace channels that were fabricated in a fused silica substrate.[9] A three-phase model was proposed to explain the transition from a bulk phase to an adsorbed phase. However, the influence of the proton-transfer layer on the actual proton transport is still unknown. According to NMR studies, an increase in the diffusion coefficient and ion mobility can be expected in the proton-transfer layer.[10] The ion mobility of protons can be related to the Grotthuss mechanism, and it can be affected by both proton hopping and by Stokes–Einstein diffusion. The increase in viscosity, which has been reported in extended nanospace, will decrease Stokes–Einstein diffusion, thus leading to a decrease in proton mobility. Therefore, it is anticipated that direct measurements of ion mobility confined to the extended nanospace fabricated in fused silica substrates will be very helpful in understanding ion mobility.

Another approach to the measurement of conductance was reported by Majumdar and Duan and involves one-dimensional nanochannels fabricated in a silicon substrate covered by a Pyrex glass.[11] The proton mobility was calculated from the conductance and a 3–4 times increase from the bulk value was seen; it was concluded that the working hypothesis would be quite different on a small scale, where nanochannels are several hundred nanometers in size. In addition, conductance is governed by both proton concentration and proton mobility, and the calculation of ion mobility is sometimes difficult. Protons supplied from the channel walls are at a concentration of 1–10 mM in channels that are smaller than 10 nm, and also contribute to enhancement of the conductance. In the 50 nm size region, Matzke and co-workers reported a one-order enhancement of proton conductance in a one-dimensional nanochannel modified with a SO_3H group to achieve a proton-exchange membrane in the extended-nanospace channel. However, the conductance measurements in the bare fused silica substrate were not reported and no detailed discussion was given on proton mobility.[12] In both of the above studies, conductance was measured by using a current–voltage curve, however these measurements included electro-osmotic flow and the analysis was complicated.

In spite of numerous thorough investigations in the 10^{-1}–10^1 nm scale, the extended nanospace has not been explored well, and the fluidic and chemistry properties are not clearly understood. The extended nanospace is a transitional phase from single molecules to normal liquid in the microspace. It plays a very important role in the discovery of basic liquid properties, and in connecting nanotechnology and microtechnology. Herein, we report the enhancement of proton mobility in water confined in two-dimensional extended-nanospace channels that are fabricated on fused silica substrates. A pH-sensitive fluorescent probe was used to monitor the proton diffusion in the extended-nanospace channels, and proton mobility was derived from the diffusion coefficient. Changes in proton mobility were observed, and this tendency was discussed in relation to the Grotthuss mechanism, in addition, the Stokes–Einstein diffusion was compared with the NMR results.

In this study, we designed and fabricated the nanochannel devices on fused silica substrates; these devices consist of two U-shaped microchannels (500 μm wide and 30 μm deep) bridged by a nanochannel network (in total 200 nanochannels, with different equivalent diameters, for each substrate with a length of 400 μm. The details of the fabrication processes for the nanochannels and the microchannels (see the Experimental Section), and the thermal bonding process were described previously.[10] The sizes of the prepared nanochannels are summarized in Table 1.

In our experimental system (Figure 1a) pressure driven control and pressure controllers were utilized,[13] and three-way valves were used to change the pressure quickly.

[*] H. Chinen, Dr. K. Mawatari, Dr. Y. Pihosh, K. Morikawa, Dr. Y. Kazoe, Prof. T. Kitamori
Department of Applied Chemistry, School of Engineering
The University of Tokyo
7-3-1 Hongo, Bunkyo, Tokyo 113-8656 (Japan)
E-mail: kitamori@icl.t.u-tokyo.ac.jp
Homepage: http://park.itc.u-tokyo.ac.jp/kitamori/top_e.htm
Dr. T. Tsukahara
Research Laboratory for Nuclear Reactors
Tokyo Institute of Technology
2-12-1-N1-32 O-Okayama, Meguro-ku, Tokyo 152-8550 (Japan)

[**] This work was supported by core research for evolutional science and technology (CREST) of Japan Science and Technology Agency (JST).

Supporting information for this article is available on the WWW under http://dx.doi.org/10.1002/anie.201104883.

Table 1: The size of nanochannels for proton diffusion measurement.

Width [nm]	Depth [nm]	Equivalent diameter D [nm][a]
190	170	180
430	270	330
490	400	440
670	500	570
850	650	740
1170	870	1000
1340	1840	1580

[a] The equivalent diameters were determined from images obtained with the scanning electron microscope and an atomic force microscopy, as an example see Figure 1 b–d.

Fluorescence microscopy was used to monitor the change in fluorescence intensity in the extended-nanospace channels. Fluorescein aqueous solutions were used for proton diffusion measurements. Fluorescein molecules have a pK_a of 6.4, and the fluorescence quantum yield becomes smaller when the pH is decreased. The linearity between the fluorescence intensity and pH was confirmed in the pH range of 2–7. We confirmed that the interface of dark (low pH) and bright (high pH) areas was clearly observed by a gradient of proton concentration between the microchannels. Several nanochannels (upper channels in the picture in Figure 2 a) could not introduce the solution because they became clogged. The interface moved at almost the same speed in all nanochannels (Movie S1 in the Supporting Information). The proton diffusion length L is related to time t by following a well-known equation,

$$L = \sqrt{2Dt} \quad (1)$$

where D is the diffusion coefficient of a proton in water. Figure 3 a shows the time dependence of fluorescent signals at different positions along the nanochannels. These data show a plateau before the pH decrease, and then a sudden decrease in fluorescence intensity was observed as a result of the pH decrease caused by proton diffusion. The intensity differences before and after the pH change became smaller for a longer L as a result of photobleaching of the fluorescein molecules. The plateau and the slope were fitted with a linear function, and the time at which the protons reached the required position was obtained by noting the time where the two linear lines crossed. Then, this proton-reaching time was plotted against L^2 values (Figure 3 b), the points were fitted with a linear function, and the proton diffusion coefficient was derived by calculating the slope of the fitted line. The correlation coefficient was 0.98, and the curve showed good linearity. The diffusion coefficient in Figure 3 b was $5.1 \times 10^{-9}\ m^2 s^{-1}$. Diffusion coefficients for various channel sizes in the range of 180–1600 nm were obtained, as shown in Figure 4.

The proton diffusion coefficient decreased for channel sizes of below 1580 nm, and enhancement started from 330 nm.. The enhancement

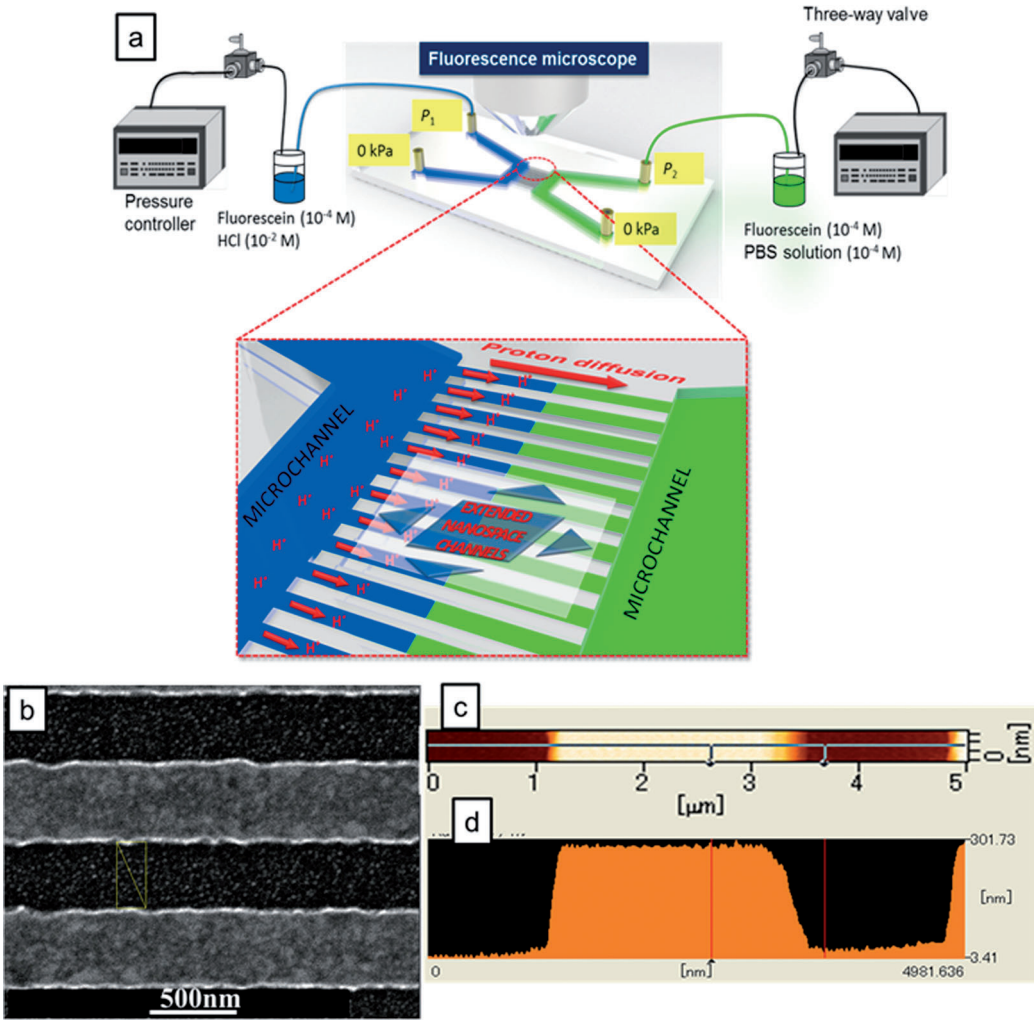

Figure 1. a) Schematic illustration of the experimental system used to measure proton diffusion in nanochannels. The nanochannel device consists of two U-shaped microchannels (500 µm wide and 30 µm deep), b) SEM image of two nanochannels with equivalent diameter of 330 nm, c) AFM image of one nanochannel and d) cross-sectional analysis of the AFM image.

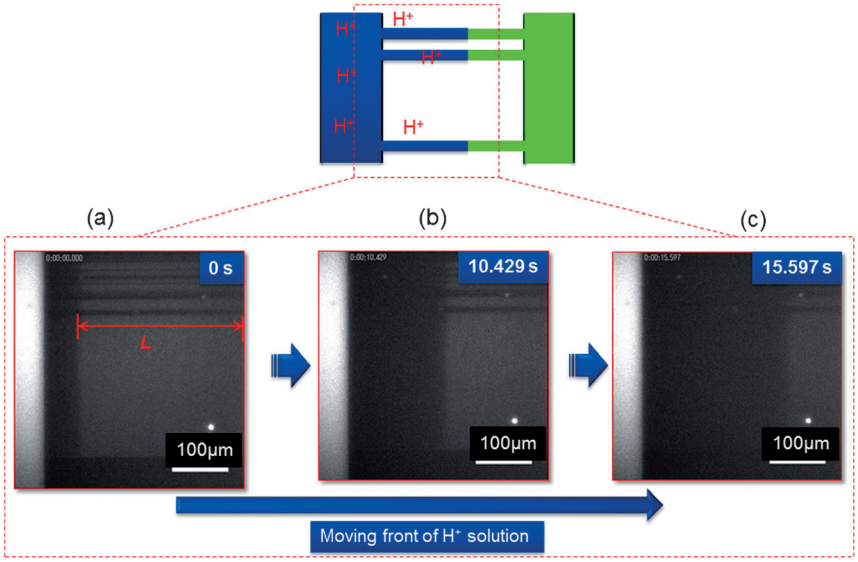

Figure 2. Proton diffusion across nanochannels ($D = 737$ nm) at $t = 0$ s (a), $t = 10.429$ s (b), and $t = 15.597$ s (c).

As proton mobility is directly related to the diffusion coefficient shown in the Einstein relation, it increases in this region. Protons show a very unique diffusion pattern based on the Grotthuss mechanism, and the diffusion coefficient can be expressed by Stokes-Einstein diffusion and proton hopping with weighing parameters of χ_S and χ_H as below,[10]

$$D = \chi_S \frac{kT}{6\pi a\eta} + \chi_H \frac{kT\lambda_{H^+}}{z^2F^2} \quad (2)$$

where z is the proton charge, F is Faraday's constant, k is the Boltzmann constant, a is the hydrodynamic radius, η is the viscosity, and λ_{H^+} is the proton mobility. From the NMR study to measure the proton-transfer rate, which corresponds to the second term in Equation (2), we observed that the value of the

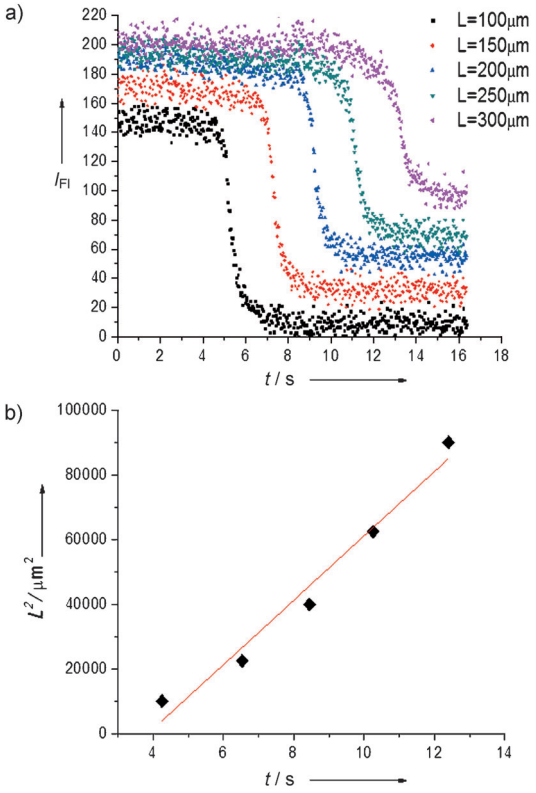

Figure 3. Result of proton diffusion measurement: a) fluorescence intensity measurement at $L = 100$, 150, 200, 250, and 300 μm (0 denotes the measurements starting point, however no changes occurred at that moment) and b) L^2/t plot to calculate the diffusion coefficient from the slope.

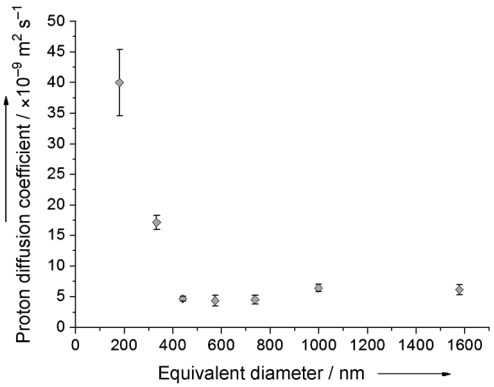

Figure 4. Proton diffusion coefficient for nanochannel sizes in the range of 180–1580 nm.

factor was observed in the nanochannel size region starting from 180 nm up to 330 nm and was almost 4 and 1.8 times higher compared with the bulk value, respectively.

second term increases with a decrease in the nanochannel size. The first term contributes to the decrease in the diffusion coefficient that occurs when the nanochannel size decreases from 1580 nm to 570 nm. Some groups reported that the viscosity of the water in nanochannels in the range of 100–1000 nm was several times higher than the vicosity of bulk water.[14,15] Based on these results, it can be concluded that an increase in the viscosity caused the decrease in the proton diffusion coefficient, and that the Stokes-Einstein diffusion was dominant in the determination of the size dependency. For a decrease in nanochannel size from 570 nm to 180 nm, the diffusion coefficient increased about 9 times (4.3 times from the bulk value, where the bulk value is 9.3×10^{-9} m^2 s^{-1}),[16,17] a result which means that the proton-hopping term increased in this region. According to the NMR study, the value of the second term increased 3–4 times,[11] and the value was comparable with the value in our experiment. The result shows that the proton-hopping process becomes dominant in this size region (570 nm–180 nm).

Previously[9,10] we have proposed a model for the proton-transfer mechanism that is supported by a three-phase theory based on the weight average of the three phases, that is, the bulk, absorbed, and intermediate phases. Specifically, the proton-transfer phase is an intermediate phase located in the extended nanochannel between the bulk phase and the absorbed phase, and plays the most important role in the enhanced proton-transfer mechanism. In the bulk phase the molecules have an ordinary liquid structure and free transplantation and rotation. In the absorbed phase the water structure is similar to ice, having a bilayer structure where both translation and rotation are inhibited. In the proton-transfer phase, the molecules have more complicated properties compared with the previous two phases: the water molecules preserve the four-coordinate H_2O structure; a slower molecular motion compared to bulk water, a size-confinement effect of only intermolecular translation without changes in rotation, proton hopping along a hydrogen-bond chain, and finally a fast proton-transfer rate induced by chemical exchange between H_2O and SiOH groups on the glass surface. Based on the NMR results, we confirmed an intermediate phase, in which protons migrate through a hydrogen-bond network and the water molecules are loosely coupled within a few tens of nanometers from the water interface and exist mainly in extended nanospace. In other words, in a proton-transfer layer, where the water molecules form a loosely structured water network (inhibited molecular motions of water) and are located within approximately 50 nm from the glass/water interface, the proton-exchange rate was enhanced owing to the hydrogen-bond network. The present study showed that the structure also contributed to the enhancement of the proton diffusion coefficient. Although Equation (2) includes three unknown parameters, these parameters can be obtained when the size dependency of the viscosity is obtained. This information is essential to investigate the ion-transport process inside nanochannels, and the traditional surface conductivity can be also well understood. The Debye length was calculated as 2–3 nm in this study and 100–300 nm (proton concentration of 10^{-5}–10^{-6} M) for the NMR study using pure water, but showed an increase in proton mobility in the both cases. This means that an electric double layer has no significant effect on the proton mobility enhancement. The conductance of the nanochannel becomes $6.4\times10^{-3}\,S\,cm^{-1}$ at 330 nm, assuming that proton concentration is 10^{-2} M, which is comparable with the Nafion membrane.[18] The proton-hopping term increases by more than 2.5 times at 40 nm, as shown by the NMR study. Then, the proton conductivity becomes $1.6\times10^{-2}\,S\,cm^{-1}$ at 40 nm. These calculations show that the nanochannels fabricated in the fused silica substrate can be an alternative to the Nafion membrane with advantages of low crossover by glass substrates and large mechanical strength.[6]

In summary, the enhancement of the proton mobility in the two-dimensional nanochannels fabricated on fused silica substrates has been verified for the first time. The proton diffusion coefficient showed a tendency to increase when the nanochannel size decreased to 330 nm, while a decrease in the proton diffusion coefficient followed an increase in viscosity, and the maximum value of the proton diffusion coefficient was observed when the nanochannel size was decreased to 180 nm. In comparison with conductance measurements, this study directly verified the increase in proton mobility in nanochannels. This new knowledge will contribute to a deeper understanding of ion-transport process inside nanochannels.

Experimental Section

Sample fabrication: As the fabrication procedures of the extended nanospace (nanochannels) and microchannels are essentially the same as those described in our previous papers[10] except for a few changes, only an outline is given here.

Extended nanospace: 0.7 mm thick fused silica substrates (VIOSILSX, ShinEtsu Quartz Co., Ltd., Tokyo, Japan) with 30×70 mm sides were coated with an electron beam resist and conductive polymer using a spin coater. Electron-beam lithography (ELS-7500, Elionix Co., Ltd., Tokyo, Japan) was used to draw an extended nanoscale pattern onto the substrates. The nanopattern drawn was developed in *o*-xylene, rinsed in 2-propanol, and fabricated by plasma etching (NE-550, ULVAC Co., Ltd., Kanagawa, Japan) using a mixture of CF_6 and CHF_3 gases. The fabricated extended nanospace consists of 200 nanochannels for each substrate with a length of 400 μm, but with 7 different equivalent diameters D (180, 330, 440, 570, 740, 1000 and 1580 nm), respectively. The sizes were determined from images obtained with a scanning electron microscope (SEM) and an atomic force microscope (AFM; SPA-400, SII NanoTechnology Inc., Chiba, Japan). The SEM and AFM images of nanospace with equivalent diameter 330 nm are shown in Figure 1b–d as an example.

Microchannels and chip fabrication: U-shaped microchannels (500 μm wide and 30 μm deep) were fabricated in other fused silica substrates by photolithography and wet etching (Institute of Microchemical Technology Co., Ltd.). These U-shaped microchannels were used to introduce solutions and were located on both sides of the extended-nanospace channels. Inlet holes were pierced through the patterned substrates using a diamond-coated drill. The substrates were then washed repeatedly in *o*-xylene, DMSO, ultrapure water, and a mixed solution of sulfuric acid and hydrogen peroxide (3:1), before being thermally laminated with the first fused silica plate (in which the extended nanospace is fabricated) in a vacuum furnace at 1080 °C (KDF-900GL, Denken Co., Ltd., Oita, Japan). As a result, the chip consists of two U-shape microchannels which are bridged by nanochannels. All operations were carried out in clean rooms (classes 100, 1000, and 10000) to exclude impurities.

Proton diffusion measurements: The pressure control protocol for protons diffusion measurement is as follows. Firstly, the fluorescein (10^{-4} M) and HCl (10^{-2} M) solution was introduced to the left microchannel at $P_1=10$ kPa, and the fluorescein (10^{-4} M) and phosphate buffer solution (PBS; 10^{-4} M) was introduced to the right microchannel at $P_2=300$ kPa (Figure 1a). Under such conditions, nanochannels were filled with the fluorescein (10^{-4} M) and PBS (10^{-4} M) solutions. Then, P_1 and P_2 were adjusted to 0 kPa to stop the flow in the microchannels; this flow was confirmed in other experiments by measuring microparticles in the solution (data not shown). Then, protons diffused from the right microchannel into the nanochannels, and the fluorescence intensity decreased owing to a pH decrease. A moving front of protons was clearly observed and recorded by a CCD camera connected to the fluorescent microscope. A PBS solution was used to prevent a large decrease in the fluorescence intensity owing to acidity in the nanochannel; however, the concentration (10^{-4} M) was much smaller than in HCl solution (10^{-2} M). Therefore, PBS did not work as a buffer solution for HCl solution, and the decrease in the fluorescence intensity during proton diffusion was clearly observed.

Received: July 13, 2011
Revised: September 20, 2011
Published online: January 25, 2012

Keywords: conducting materials · fluidics · fuel cells · nanotechnology · proton mobility

[1] P. Gallo, M. A. Ricci, M. Rovere, *J. Chem. Phys.* **2002**, *116*, 342–346.
[2] L. D. Gelb, K. E. Gubbins, R. Radhakrishnan, M. Sliwinska-Bartkowiak, *Rep. Prog. Phys.* **1999**, *62*, 1573–1659.
[3] H. Daiguji, *Chem. Soc. Rev.* **2010**, *39*, 901–911.
[4] T. Tsukahara, K. Mawatari, T. Kitamori, *Chem. Soc. Rev.* **2010**, *39*, 1000–1013.
[5] P. Abgrall, N. T. Nguyen, *Anal. Chem.* **2008**, *80*, 2326–2341.
[6] Q. Pu, J. S. Yun, H. Temkin, S. R. Liu, *Nano Lett.* **2004**, *4*, 1099–1103.
[7] A. Hibara, S. Takumi, H.-B. Kim, M. Tokeshi, T. Ooi, M. Nakao, T. Kitamori, *Anal. Chem.* **2003**, *36*, 605–612.
[8] N. Kaji, R. Ogawa, A. Oki, Y. Horiike, M. Tokeshi, Y. Baba, *Anal. Bioanal. Chem.* **2006**, *386*, 759–764.
[9] T. Tsukahara, A. Hibara, Y. Ikeda, T. Kitamori, *Angew. Chem.* **2007**, *119*, 1199–1202; *Angew. Chem. Int. Ed.* **2007**, *46*, 1180–1183.
[10] T. Tsukahara, W. Mizutani, K. Mawatari, T. Kitamori, *J. Phys. Chem. B* **2009**, *113*, 10808–10816.
[11] C. Duan, A. Majumdar, *Nat. Nanotechnol.* **2010**, *5*, 848–851.
[12] S. Liu, Q. Pu, L. Gao, C. Korzeniewski, C. Matzke, *Nano Lett.* **2005**, *5*, 1389–1393.
[13] T. Tsukahara, K. Mawatari, A. Hibara, T. Kitamori, *Anal. Bioanal. Chem.* **2008**, *391*, 2745–2752.
[14] See Ref. [7].
[15] See Ref. [8].
[16] G. W. C. Kaye, T. H. Laby, *Tables of physical and chemical constants*, Longman, London, **1973**.
[17] P. Atkins, J. Paula, *Physical chemistry*, W. H. Freeman and Co., San Francisco, **2009**.
[18] U. Sen, A. Bozkurt, A. Ata, *J. Power Sources* **2010**, *195*, 7720–7726.

